Statistic-based method to monitor belt transmission looseness through motor phase currents

Antoine Picot, Etienne Fournier, Jérémi Regnier, Mathias Tientcheu Yamdeu, Jean-Marie Andréjak, Pascal Maussion

Statistic-Based Method to Monitor Belt Transmission Looseness Through Motor Phase Currents

Antoine Picot, Etienne Fournier, Jérémi Régnier, Mathias TientcheuYamdeu, Jean-Marie Andréjak, and Pascal Maussion

***Abstract*—Belt–pulley systems are widely used in the industry due to their high efficiency and their low cost. However, only few works exist about the monitoring of their degradation. This paper details the impact of belt looseness on electrical measurements under steady and transient state in order to identify spectral signatures. This analysis enlightens the advantage of the transient state to detect belt looseness because it exacerbates belt slip. An innovative methodology is then proposed based on the application of a square-wave speed reference in order to monitor belt looseness. A statistical-based indicator is defined from the phase currents in order to automatically detect drifting of the indicator. A normalization process is also applied to increase the detection robustness. The proposed indicator is evaluated on a 30-kW induction machine and a direct-current machine coupled with two trapezoidal belts for three speed and four load conditions. It reaches very good results with almost 90% correct detections for 1% false alarms. These results are way better than those obtained with a classic spectral analysis during the steady state. Moreover, results demonstrate that higher load conditions are more accurate for the monitoring of belt looseness.**

***Index Terms*—Belt–pulley systems, fault diagnosis, induction motors (IMs), robustness, spectral analysis, statistical-based indicator, torque–speed segmentation.**

NOMENCLATURE

$\delta\Omega$	Speed square-wave peak-to-peak amplitude.
Ω	Motor speed.
σ_n	Standard deviation of coefficients c_n.
c_n	Fourier series coefficient at rank n.
d_i	Center distance between motor and load.
f_b	Rotation frequency of the belts.
f_c	Square-wave frequency.
f_f	Supply frequency.
f_l	Rotation frequency of the load.
f_r	Rotation frequency of the induction motor.
f_s	Sampling frequency.
i_1, i_2, i_3	Motor phase currents.
ia	Currents instantaneous amplitude.
if	Currents instantaneous frequency.
m_n	Average of coefficients c_n.
$X(f)$	Fourier transform of the variable $x(t)$ at frequency f.

Color versions of one or more of the figures in this paper are available online at http://ieeexplore.ieee.org.
Digital Object Identifier 10.1109/TII.2017.2661317

I. Introduction

INDUSTRIAL systems' maintenance has become an important economical issue over the past years. The dependence between machines and production lines makes electromechanical systems one of the critical elements of industrial plants. Their failure may indeed provoke unexpected production shutdowns and important safety issues. In this context, many diagnosis strategies have been developed to monitor electrical machines.

Studies have mainly focused on the diagnosis of faults directly related to the electrical motors such as bearing faults [1]–[3], rotor faults [4]–[6], or winding faults [7]–[9]. If vibration signals were first used as a robust indicator for the monitoring of electrical machines [10]–[12], recent studies would have mainly focused on the processing of electrical measures such as phase currents since they are often available for control purposes. The main technique used for the monitoring of electrical machines is probably the exploitation of frequential signatures induced by different faults. This technique is known as motor current signature analysis (MCSA), and a review of different techniques can be found in [13]. A lot of different signal processing tools have been explored to extract and track specific fault components such as the Fourier transform, the wavelets transform, or the empirical mode decomposition, with similar performance. A complete state of the art can be found in [14]. However, less attention has been paid to the monitoring of a transmission system such as gears of belt–pulley drives. In these cases, MCSA techniques are often limited [15] due to the fact that signatures are distorted by the transmission system and original techniques must be developed.

Belt–pulley systems are extensively employed in industrial applications such as compressors, pumps, fans, etc. The main advantages of belt transmission are its high efficiency, the non-necessity of aligned shafts, its tolerance for misalignment, and its low cost [16]. They are generally composed of two pulleys, one or several belts, and eventually other mechanical elements (tension roller, guide roller, etc.). The most popular types of belts are the flat and trapezoidal ones (also known as V-belts). Belt transmission systems working under degraded conditions can, therefore, lose their mechanical properties over time and lead to belt rupture, severe pulleys wear, or excessive belt slip [17], [18]. Among different failure modes, belt looseness is an important issue. Indeed, it increases the belt slip and thus accelerates the wear process of the transmission system [19]. Recent study [20] has focused on the effects of belt looseness on a system driven by an induction motor (IM). This work concluded that phase currents were sensitive to belt looseness conditions and that the belt slip were exacerbated when applying a speed step reference to the motor, implying that the transient state was more interesting for diagnosis purpose.

This work presents a belt looseness indicator based on the analysis of the transient state of a belt–pulley system driven by an IM. This strategy was recommended in [20]. Since this indicator must be suitable for industrial applications, it must be able to adapt itself to the application, so it does not have to be extensively tuned by the operator. Recent works [2], [21] have shown that statistical processing of the data could be an interesting approach to automatically detect a drifting of the parameters. Moreover, it must also be able adapt to the load condition, since it seems not realistic to suppose that the belt–pulley system (such as pumps or fans) will work under a single load during its lifetime. In order to overcome this point, Fournier *et al.* have shown in [22] that an adequate segmentation of the torque–speed plane helps to increase the robustness of the monitoring. We propose here to use this strategy with a proper belt looseness indicator in order to develop a robust monitoring system for belt transmission application. The proposed monitoring scheme has been designed in partnership with the machine manufacturer Leroy Somer in order to be acceptable for a wide range of applications working in open-loop condition such as compression, ventilation, and pumping processes.

The outline of this paper is the following. The belt transmission system used in this study is presented in Section II. The degradation protocol and different measures are detailed in this section. The effects of belt looseness on electrical measures for steady and transient states are presented in Section III. This section sums up work presented in [20] and focuses on the use of the instantaneous frequency to monitor the system. The relevancy of different frequency signatures is studied in this section. A monitoring method is then proposed in Section IV. This method is based on the use of a small transient state to increase the effect of belt looseness. In order to make the proposed indicator robust to load variations, a torque–speed mapping protocol inspired by Fournier *et al.* [22] is also proposed. Section V details the results for different load conditions and transmission ratios. These results are compared to those obtained in the steady state and discussed.

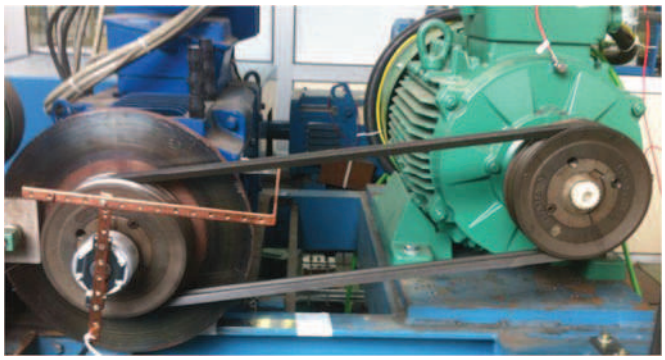

Fig. 1. Experimental test bench composed of an 30-kW IM (right), a belt–pulley transmission system (middle), and a direct-current machine (left).

II. Belt Transmission System

A. Test Bench Presentation

The experimental test bench used in this study is displayed in Fig. 1. It has been developed in association with Leroy Somer. This test bench is composed of the following:

1) a squirrel-cage IM with one pair of poles, a rated power of 30 kW, and a rated speed of 2946 r/min;
2) a transmission system composed of two 160-mm-diameter pulleys and two trapezoidal belts with a length of $L_{\text{belts}} = 1600$ mm (Texrope VP2 1600 SPA);
3) a direct-current machine used to vary the torque delivered by the IM.

The IM is fed by a pulse-width-modulated inverter with a constant V/f open-loop control law. This way, it is possible to control the IM speed (neglecting the slip) by imposing the stator current frequency. This control mode is widely used for different kinds of applications, and Leroy Somer estimates that about 90% of their IMs sold are used with this control mode. The center distance d between the load machine and the IM can be adjusted in order to increase or decrease belts tension. Tests can thus be carried out for healthy conditions, with a proper tension of the belts, and for faulty conditions by gradually decreasing the distance d between the motor and its load. In this test bench, the diameters of the driven pulley D_{driven} and the driver pulley D_{driver} are equal. The transmission ratio $R_t = D_{\text{driven}}/D_{\text{driver}}$ is then equal to 1. This ratio has been chosen in order to simplify the analysis of different results during the description of the proposed method. Results for a nonunitary ratio are presented in Section V in order to confirm the performance of the proposed indicator in a more realistic case.

B. Measurements

An eight-synchronous-channel data acquisition system has been used to record mechanical and electrical signals with a sample frequency $f_s = 100$ kHz. Different recorded data are the following:

1) the radial and axial vibration signals (respectively, γ_r and γ_a) via two accelerometers (Dytran 3055A2) placed on the motor frame;

TABLE I
CENTER DISTANCES AND RELATED BELTS CONDITION USED DURING THE EXPERIMENTAL TESTS

Center distance	Belts condition
d_1	Healthy belts
d_2	Moderate belt looseness
d_3	Strong belt looseness
d_4	Critical belt looseness

2) the motor and load mechanical speed signals (respectively, Ω_{motor} and Ω_{load}), thanks to two encoders;
3) the motor phase currents i_1, i_2, and i_3.

All recordings have the same length T_{rec} equal to 5 s. The belt slip, noted S_Ω, is calculated from Ω_{motor} and Ω_{load} according to

$$S_\Omega = \Omega_{\text{motor}} - R_t.\Omega_{\text{load}} \quad (1)$$

with R_t being the transmission ratio. It can also be defined in relative terms by

$$s_\Omega = \frac{S_\Omega}{\Omega_{\text{motor}}} \cdot 100 \quad (2)$$

for all measurements.

Four different center distances have been tested from d_1 to d_4. These distances correspond to different belt looseness conditions represented in Table I.

The center distance d_1 is the correct belt tension, which ensures an optimal functioning of the system. On the contrary, the center distance d_4 provokes a critical looseness of the belts, which even prevents the system to work under the rated load and speed. Two intermediate center distances d_2 and d_3 have also been tested between these two extreme cases. They, respectively, induce moderate and strong belt looseness.

Tests have been carried out for at half the nominal speed ($\Omega_n/2 \simeq 1500$ r/min) for five different load conditions of the IM. The load conditions are $I_0 \simeq 15$ A, $I_n/2 \simeq 26$ A, $3I_n/4 \simeq 38$ A, $7I_n/8 \simeq 45$ A, and $I_n \simeq 52$ A, with I_0 the no-load condition and I_n the nominal load condition. More tests have been carried out for the evaluation of the proposed method. They are described in Section V-A.

III. EFFECTS OF BELT LOOSENESS ON ELECTRICAL MEASURES

A. Effects on Belt Slip

The relative belt slip s_Ω has been computed for each load condition according to (2). It is supposed to increase with the belt looseness because of the loss of adhesion. Moreover, its spectral content should be affected by torque oscillations due to belt flapping.

Fig. 2 displays the evolution of the belt slip depending on the looseness for different load conditions. Darker colors correspond to higher load conditions. It can be seen in this figure that the average belt slip is increasing with the looseness. Its value is about 2% of the motor speed with healthy belts whatever the load condition. The relative slip reaches, however, higher value (till 8% of the motor speed) in the critical condition. The effect

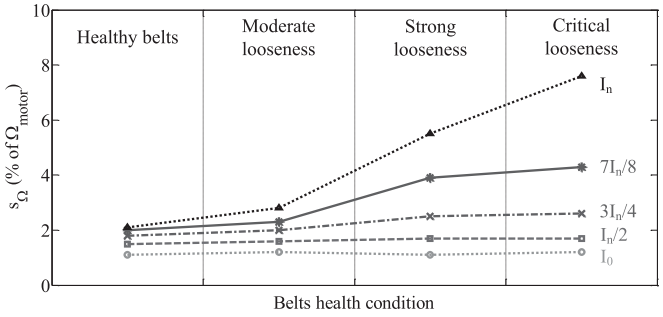

Fig. 2. Evolution of relative belt slip s_Ω with the load condition at $\Omega = 1500$ r/min.

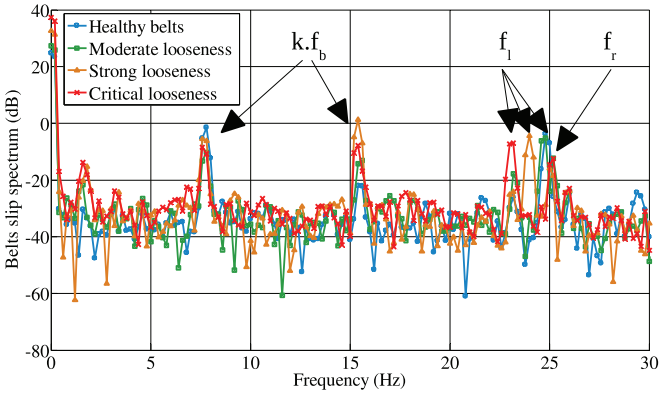

Fig. 3. Belt slip spectrum for different looseness conditions at $I_n = 52$ A and $\Omega = 1500$ r/min.

of the looseness is especially obvious as the load condition increases. It can be concluded that it is better to use a high-load condition in order to observe belt slip. In this case, belt slip seems to be a relevant indicator of belt looseness.

The belt slip spectrum has also been computed for different looseness conditions at $I_n = 52$ A. The results are plotted in Fig. 3. Higher looseness corresponds to warmer colors. Three harmonic families can be noticed in this spectra: one depending on the rotation frequency of the belts f_b, one depending on the rotation frequency of the load f_l, and one depending on the rotation frequency of the motor f_r. Here, f_r and f_l are almost the same due to the fact that the ratio 1:1 is used for the transmission.

The belt rotation frequency f_b can be defined according to (3) in the case of no slip between the belts and the motor pulleys. In this equation, L_b is the length of the belts and D_m is the motor pulley diameter:

$$f_b = \frac{\pi.D_m}{L_b} \cdot f_r. \quad (3)$$

It can be seen in Fig. 3 that harmonics multiples of f_b such as $S_\Omega(f_b)$ and $S_\Omega(2.f_b)$ are affected by the belt looseness: $S_\Omega(f_b)$ is decreasing, while $S_\Omega(2.f_b)$ is increasing with the looseness. The harmonic $S_\Omega(f_l)$ is also impacted by the increase of the looseness. Its value seems to remain the same, but its position changes with the looseness. This can be explained by its

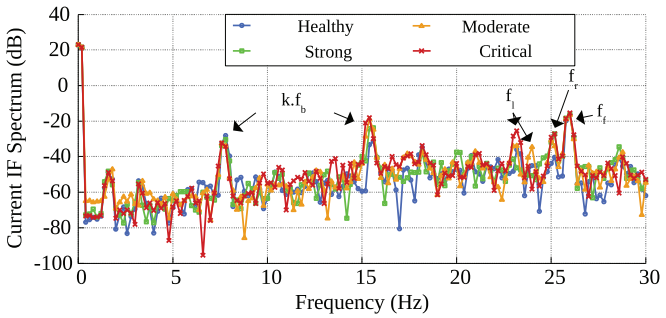

Fig. 4. Evolution phase currents instantaneous frequency spectrum $|\mathrm{IF}(f)|$ with the looseness severity for $I_n = 52$ A and $\Omega = 1500$ r/min.

definition (4), with $< s_\Omega(t) >$ being the average value of the relative belt slip. The belt slip obviously impacts the value of f_l, which explains the frequential shift with the looseness

$$f_l = (1 - < s_\Omega(t) >) \cdot f_r. \tag{4}$$

The harmonic $S_\Omega(f_r)$ seems to increase for strong and critical belt looseness. It is, however, difficult to tell in the case of looseness of healthy belts and moderate belts, since they are very close to $S_\Omega(f_l)$.

B. Effects Under Steady-State Operation

Fournier *et al.* have demonstrated in [20] that belt looseness had a strong impact on mechanical variables such as motor speed or vibration signals. Nonetheless, it is more convenient to use electrical variables for the monitoring since speed or vibration sensors are expensive and electrical quantities (such as phase currents) are often already accessible through the speed drive for control purposes. Belt looseness induces speed oscillations that impact the spectral content of phase currents.

Instantaneous frequency is well fitted for the monitoring of torque oscillation [23]. The phase current instantaneous frequency $\mathrm{if}(t)$ has been computed by the Concordia transform on the data. Their power spectra $|\mathrm{IF}(f)|$ are displayed in Fig. 4. Higher looseness corresponds to warmer colors.

It can be seen in Fig. 4 that the same frequency families as those identified in Section III-A are modified with belt looseness. The frequency multiples of f_b, f_l, and f_r are impacted by belt looseness. Their behavior seems to be very similar to the one of the corresponding harmonics in the belt slip spectrum. A modeling of the electromechanical system would be necessary here to perfectly understand the connection between the dynamic of the belt and the stator current, which is not the purpose of this paper.

Three harmonic families are likely to allow the monitoring of belt looseness. Nevertheless, belt slip and load speed are usually not measured on industrial drives. The rotation frequency seems then the only suitable candidate for belt looseness monitoring. So, a first indicator of belt looseness is the evolution of $|\mathrm{IF}(f_r)|$. The mean increase of this indicator from its healthy value has been computed for each belt condition. Table II displays these values for different operating points.

TABLE II
EVOLUTION OF THE CURRENT INSTANTANEOUS FREQUENCY HARMONIC $\mathrm{IF}(f_r)$ AVERAGE VALUE WITH THE BELT LOOSENESS SEVERITY FOR DIFFERENT LOAD CONDITIONS AT $\Omega = 1500$ R/MIN

Load level	Moderate looseness	Strong looseness	Critical looseness
$I_0 \simeq 15$ A	+1 dB	+0 dB	+0 dB
$I_n/2 \simeq 26$ A	+12 dB	+17 dB	+18 dB
$3I_n/4 \simeq 39$ A	+10 dB	+17 dB	+16 dB
$7I_n/8 \simeq 45$ A	+11 dB	+16 dB	+17 dB
$I_n \simeq 52$ A	+10 dB	+14 dB	+14 dB

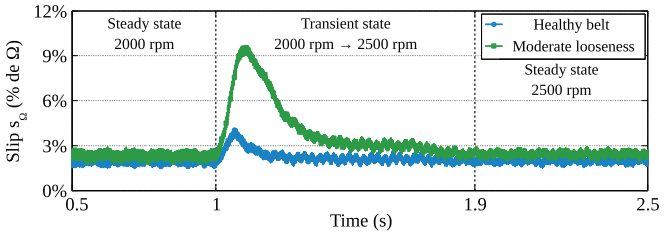

Fig. 5. Relative belt slip response to the speed reference step for healthy and loosen belts under the load level $I = 38$ A.

The results shown in Table II demonstrate that $|\mathrm{IF}(f_r)|$ is suitable for belt looseness detection because its value increases in the case of belt looseness (compared to the healthy case). It seems, however, unable to monitor the fault severity, since there is not much difference between strong and critical looseness. Moreover, a minimal load torque is necessary to observe this difference. The level of $|\mathrm{IF}(f_r)|$ is not impacted by the tension loss in the no-load condition ($I_{\mathrm{motor}} = I_0$).

C. Effects Under Transient-State Operation

Although belt looseness has a clear influence on the phase currents under steady operation, as shown in Section III-B, Fournier *et al.* have demonstrated in [20] that belt slip is exacerbated when sudden accelerations are imposed to the system. Fig. 5 displays the temporal response of the relative belt slip when applying a speed step rising from 2000 to 2500 r/min at $t = 1$ s for looseness of healthy belts (green) and moderate belts (blue).

It can be seen in Fig. 5 that the relative slip is slightly greater for moderate belt looseness than for healthy belts during steady states at $\Omega = 2000$ r/min and $\Omega = 2500$ r/min. This is consistent with results presented in Section III-A. Moreover, it is obvious from Fig. 5 that the relative belt slip is strongly increased during the transient state because it reaches almost 10% for moderate belt looseness against 4% only for healthy belts.

The effect of belt slip is clearly visible on the instantaneous amplitude $\mathrm{ia}(t)$ of the phase currents computed by the Concordia transform, as displayed in Fig. 6.

It can be noticed in Fig. 6 that response of $\mathrm{ia}(t)$ during the transient state is distorted with belt looseness. Its amplitude peak is attenuated in the first part of the step response, and the drop is slower when loosen belts are used instead of healthy belts. It seems nevertheless difficult to impose such an acceleration in

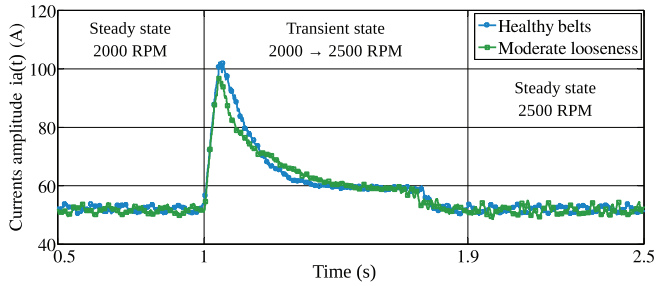

Fig. 6. Dynamic response of motor current instantaneous amplitude $\mathrm{ia}(t)$ to the speed reference step for healthy and loosen belts under the load level $I = 38$ A.

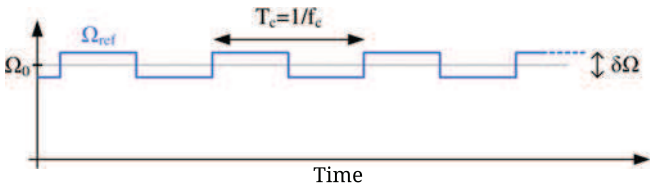

Fig. 7. Proposed speed profile formed by the superposition of constant speed reference Ω_0 and a speed square input $\delta\Omega/2$ at frequency f_c.

real-life applications in order to produce a fault signature related to the belt condition.

IV. Belt Looseness Monitoring Method

A. Effect of a Square Waveform Speed Reference

According to the results presented in Section III, the effects of belt looseness are exacerbated under transient-state operation due to the motor acceleration, which makes them easier to monitor. Unfortunately, it seems inconceivable to use a strong speed step reference (as presented in Section III-C) since the application would be greatly impacted and might not tolerate it or to diagnose the system only when it is turned ON.

The solution proposed in this paper is to add a low-speed square input $\delta\Omega$ to a constant speed reference Ω_0 (with $\delta\Omega << \Omega_0$) in order to provoke slight transients and reproduce the effects of a speed step reference with a known period T_c. The proposed speed profile is presented in Fig. 7. It is possible to impose such a profile because the IM is driven with a constant V/f open-loop control law. The amplitude of $\delta\Omega$ must be low enough not to impact the application working. The period T_c must be long enough to observe the impact of the motor acceleration and short enough to observe a large number of accelerations during the recording duration T_{rec}. This profile has been defined in partnership with the motors' manufacturer Leroy Somer in order to be acceptable for a wide range of applications such as compression, ventilation, and pumping processes.

The effect of such a speed profile will impact periodically the belt slip and so the instantaneous frequency $\mathrm{ia}(t)$. Since the effect of belt slip appears with a period T_c on $\mathrm{ia}(t)$, it can then be expressed as a Fourier series according to the following

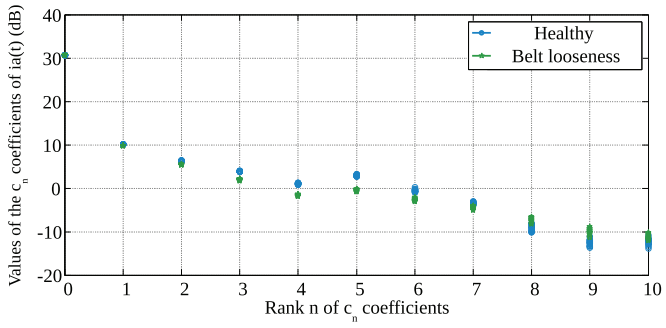

Fig. 8. Values of the c_n coefficients for the instantaneous amplitude of the phase currents for healthy and faulty belt conditions at $7I_n/8 = 45$ A and $\Omega_0 = 2000$ r/min.

equation:

$$\mathrm{ia}(t) = \sum_{n=0}^{+\infty} c_n \cdot \cos(2\pi n f_c t + \phi_n). \tag{5}$$

The coefficients c_n characterize the amplitude of the harmonic response of $\mathrm{ia}(t)$ to the square speed profile. Their values will then be modified if $\mathrm{ia}(t)$ is modified. Moreover, these coefficients can be estimated as $|\mathrm{IA}(n \cdot f_c)|$, the values of the Fourier transform of $\mathrm{ia}(t)$ at multiple of the known frequency $f_c = 1/T_c$, and used as fault signatures.

Fig. 8 represents the values of different coefficients $c_n = |IA(n \cdot f_c)|$ for n from 1 to 10 for healthy belts (blue circles) and for moderate belt looseness (green stars). These results have been obtained by applying the proposed speed profile with a period $T_c = 1$ s and a speed square waveform of peak-to-peak amplitude $\delta\Omega \simeq 55$ r/min added to a speed reference $\Omega_0 = 2000$ r/min. Note that $\delta\Omega$ is less than 2% of the motor nominal speed $\Omega_n = 2946$ r/min, which should not impact much real-life applications.

Fig. 8 shows that the coefficients of the Fourier series are impacted by the increase of the belt looseness. A decrease of harmonics from 2 to 7 and an increase of harmonics from 8 to 10 can be noticed. These changes reflect the distortion of $\mathrm{ia}(t)$ with the proposed speed profile. They can, thus, be used as indicators of belt looseness.

B. Proposed Indicator

Since c_n coefficients are varying along with belt looseness, the purpose is to detect their significant variations in order to discriminate belt looseness cases from healthy cases. Picot *et al.* have presented a method to normalize the fault signature in [2] in order to enlighten meaningful variations. This approach is based on the computation of the mean and the standard deviation of the fault signature during the healthy functioning of the machine. Abnormal behavior of the machine can thus be detected by applying a statistical t-test.

The same process is applied to normalize each c_n coefficient. The average m_n and the standard deviation σ_n are computed from the first N_{ref} recordings. Normalized signatures $c_{\text{CR}}(n)$ are then computed for each new recording, thanks to the following

equation:

$$c_{\text{CR}}(n) = \frac{|c_n - m_n|}{\sigma_n}. \tag{6}$$

The coefficients $c_{\text{CR}}(n)$ are close to 0 in healthy cases because m_n and σ_n are computed with a healthy belt and should be increasing in faulty cases due to the drift of the c_n value from the healthy one. The variable $c_{\text{CR}}(n)$ is supposed to follow a standard normal distribution $\mathcal{N}(0, 1)$, and a detection threshold depending on the number N_{ref} of recordings used to compute the healthy reference can then be statistically defined.

It can be seen in Fig. 8 that the impact of belt looseness on c_n coefficients is spread on different coefficient levels and not focused on a specific one. It means a large number signatures $c_{\text{CR}}(n)$ to monitor. We propose to merge these different signatures in order to get a single fault indicator. A fault indicator X_{CR} is thus defined as a linear combination of signatures $c_{\text{CR}}(n)$ according to (7). The weight of each $c_{\text{CR}}(n)$ is chosen decreasing with n because it has been shown in Section III-C that belt looseness affects mainly the low frequencies

$$X_{\text{CR}} = \frac{\sum_{n=1}^{n_{\text{lim}}} \frac{1}{n} c_{\text{CR}}(n)}{\sum_{n=1}^{n_{\text{lim}}} \frac{1}{n}}. \tag{7}$$

In the following, the number of considered signatures is set to $n_{\text{lim}} = 10$. This number has been chosen empirically in order to have enough coefficient so the indicator is stable. Adding more coefficients does not impact too much the indicator due to the $1/n$ weighting.

C. Diagnosis Process

Belt transmission systems are widely used in industrial applications such as compressors, pumps, or fans. Their load condition can then change during their lifetime and seems difficult to impose. Unfortunately, the fault indicator value might change with the load condition even in healthy cases. In order to overcome this issue and increase the reliability of the indicator, Fournier *et al.* have presented a promising technique in [22] based on the torque–load plan segmentation. The idea is to segment the torque–load plan in several zones in order to compute a healthy reference by zone. This way, when the diagnosis is processed, it is compared to the healthy reference of corresponding load and torque, and the proposed indicator will work even if machine changes its load conditions during its lifetime.

Here, the torque–load plan has been divided into 50 zones according the recommendations of [22]. Five diagnosis speeds have been chosen from $\Omega_1 = 300$ r/min to $\Omega_5 = 2700$ r/min every 600 r/min. Ten load conditions have been chosen at every 6 A. For each diagnosis phase, the speed is set to the closest diagnosis speed, so the application is not too much impacted by the diagnosis. During the machine lifetime, the diagnosis phase is processed regularly. At the beginning, the indicator values are used to compute the healthy reference, supposing that the application is correctly functioning. Once a sufficient number of measures have been obtained to compute a healthy reference for a zone, the zone is considered as active and can be diagnosed. After a certain amount of time, the learning part is considered to be over in order not to used faulty cases to build the healthy reference. Sectors that are not active will be impossible to diagnose. Algorithm 1 details the diagnosis process over different zones.

Algorithm 1: Diagnosis Process.

```
while Application lifetime do
  if Diagnosis phase then
  Speed estimation Ω_e
  Speed set to the closest diagnosis speed Ω_i
  Sector definition
  Measurement
  Speed back to Ω_e
  Computation of c_CR(n)
   if Sector is "active" then
   Computation of X_CR
   if X_CR > threshold then
    Alarm
   end if
  else
   Computation of m_n and σ_n
   if Enough measurements then
    Sector is set to "active"
   end if
  end if
 end if
end while
```

V. Results and Discussion

A. Evaluation Protocol

The proposed methodology has been evaluated on the experimental bench presented in Section II-A. Healthy (d_1), moderate (d_2), and strong (d_3) belt looseness has been tested. Critical belt looseness (d_4) has not been evaluated here because the belt slip was too strong for the application to work. Several load–torque conditions have been explored in order to simulate the functioning of a compressor-like application. It corresponds to $\Omega_3 = 1500$ r/min, $\Omega_4 = 2100$ r/min, and $\Omega_5 = 2700$ r/min, and to $I_5 = 26$ A, $I_8 = 38$ A, $I_9 = 45$ A, and $I_{10} = 52$ A. So, a total of 12 sectors have been tested.

A total number of 960 recordings have been performed in condition d_1. These recordings will allow the computation of the healthy references in different conditions and also the evaluation of the indicator in healthy cases with data different than those used for the reference. For faulty conditions, 360 recordings have been done in each belt condition d_2 and d_3. The number of recordings used to compute the healthy reference is set to $N_{\text{ref}} = 50$. All recordings have a length of 5 s. Three indicators are evaluated in this section:

1) $|\text{IF}(f_r)|$, the instantaneous frequency at f_r under the steady state (cf., Section III-B);
2) $\text{IF}_{\text{CR}}(f_r)$, the instantaneous frequency at f_r under the steady state with the normalization process presented in Section IV-B;

3) X_{CR}, the proposed indicator using a square-wave speed reference.

The detection threshold used for each indicator is a 1% detection threshold and is noted $t_{1\%}$. It is defined as the value which guarantees a maximum of 1% detection in the healthy condition, i.e., 1% false alarms. This threshold is empirically defined for $|\text{IF}(f_r)|$ and statistically defined for $\text{IF}_{\text{CR}}(f_r)$ and X_{CR}. Three criteria are used to evaluate different indicators:

1) FA, the percentage of false alarms in the healthy condition;
2) TD(d_2), the percentage of good detections for moderate belt looseness;
3) TD(d_3), the percentage of good detections for strong belt looseness.

Another test campaign has been run in order to evaluate the proposed indicator with a nonunitary ratio. The diameters of the driver pulley and the driven pulley used in this campaign are, respectively, $D_{\text{driver}} = 250$ mm and $D_{\text{driven}} = 160$ mm, which implies a transmission ratio $R_t \simeq 1.56$. The length of the belts has also been changed to $L_{\text{belts}} = 1757$ mm in order to adapt to the new configuration. Recordings have been done in the case of healthy belt (d_1) and strong belt looseness (d_3). The same torque–load conditions were explored than in the first test campaign except for Ω_5. This speed would have needed to increase the IM speed to 4212 r/min, which is higher than its nominal value. A total number of 1280 recordings were performed in this second campaign: half in the d_1 condition and half in the d_3 condition.

B. Results

The diagnosis process presented in Section IV-C has been applied to different recordings. The three indicators are displayed in Fig. 9. $|\text{IF}(f_r)|$ is pictured in (a), $\text{IF}_{\text{CR}}(f_r)$ in (b), and X_{CR} in (c). The threshold $t_{1\%}$ is depicted in red. The signatures are displayed in function of the recording number. In each belt condition, lower recording number corresponds to lower load condition. The vertical lines corresponds to condition changes (load or speed).

The detection results are summed up in Table III for different indicators.

Tables IV and V detail the results obtained with the proposed indicatorss for each speed–torque condition for moderate and strong belt looseness, respectively.

Table VI displays the results obtained with a nonunitary transmission ratio. Results obtained with $\text{IF}_{\text{CR}}(f_r)$ and X_{CR} only are presented because it can be seen from Table III that $|\text{IF}(f_r)|$ has poor performance.

C. Discussion

The analysis of Fig. 9 shows that the raw indicator $|\text{IF}(f_r)|$ is not well suited for robust detection all over the torque–load plan. It is very noisy, and its value in the healthy condition varies in such a way that it is sometimes higher in the healthy condition than for moderate or strong belt looseness. This is not the case for the normalized indicators. Their value is close to zero during the healthy functioning and increase only in the case of belt looseness. This point illustrates one of the advantages of the proposed method. The normalization step ensures that the healthy values are close to zero, and the torque–speed plan segmentation ensures that this is the case whatever the load and speed conditions. Thus, only the significant increases are enlightened by the indicators, corresponding to belt looseness. The blanks of the normalized indicators correspond to the learning of the healthy reference for each sector. Moreover, it is interesting to note that the proposed indicator reacts more proportionally with belt looseness than $\text{IF}_{\text{CR}}(f_r)$. This confirms that the use of the transient state is better to observe belt looseness rather than the steady state.

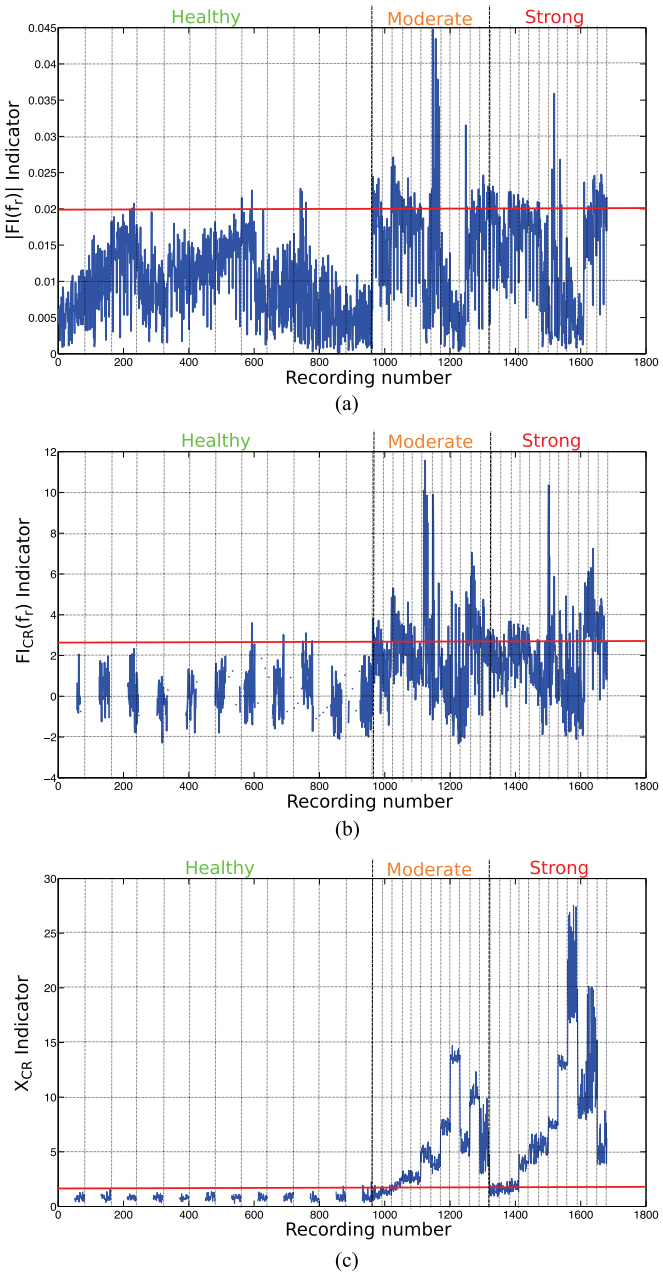

Fig. 9. Evolution of (a) $|\text{IF}(f_r)|$ indicator, (b) $\text{IF}_{\text{CR}}(f_r)$ indicator, and (c) X_{CR} indicator with the $t_{1\%}$ threshold in red for healthy belt and moderate belt looseness, and strong belt looseness.

TABLE III
RESULTS OF DIFFERENT INDICATORS (UNITARY RATIO)

Indicator	Healthy belts	Moderate looseness	Strong looseness
$\lvert \mathrm{IF}(f_r) \rvert$	FA $= 1.1\%$	TD$(d_2) = 23.6\%$	TD$(d_3) = 21.4\%$
$\mathrm{IF}_{\mathrm{CR}}(f_r)$	FA $= 1.7\%$	TD$(d_2) = 43.3\%$	TD$(d_3) = 45.0\%$
X_{CR}	FA $= 1.4\%$	TD$(d_2) = 85.8\%$	TD$(d_3) = 89.2\%$

TABLE IV
DETECTION RATE FOR THE PROPOSED INDICATOR—MODERATE BELT LOOSENESS

		Speed		
		Ω_3	Ω_4	Ω_5
Load	I_5	10%	20%	76%
	I_8	100%	100%	100%
	I_9	100%	100%	100%
	I_{10}	100%	100%	100%

TABLE V
DETECTION RATE FOR THE PROPOSED INDICATOR—STRONG BELT LOOSENESS

		Speed		
		Ω_3	Ω_4	Ω_5
Load	I_5	27%	57%	70%
	I_8	100%	100%	100%
	I_9	100%	100%	100%
	I_{10}	100%	100%	100%

TABLE VI
RESULTS OF DIFFERENT INDICATORS (NONUNITARY RATIO)

Indicator	Healthy belts	Strong looseness
$\mathrm{IF}_{\mathrm{CR}}(f_r)$	FA $= 0.4\%$	TD$(d_3) = 6.1\%$
X_{CR}	FA $= 1.3\%$	TD$(d_3) = 98.7\%$

The results of Table III show that there are 1% false alarms in all cases. These is normal because the threshold has been chosen in order to guarantee 1% false alarms. In the case of the normalized indicators $\mathrm{IF}_{\mathrm{CR}}(f_r)$ and X_{CR}, the percentage of false alarms is slightly greater than 1%. This is explained by the fact that the threshold value has been chosen *a priori*, according to statistic laws. So, the experimental results confirm 1%. This point is very important because it demonstrates that the detection threshold can be chosen *a priori* without any information on the indicator healthy values or on the application. This is another advantage of the normalization step. The torque–speed segmentation ensures that the normalization is done in every sector in order to increase the selectivity.

The detection results of Table III confirm the visual analysis. The proposed method reaches excellent results with more than 85% of correct detections of moderate belt looseness and almost 90% detections of strong belt looseness. The normalized steady indicator $\mathrm{IF}_{\mathrm{CR}}(f_r)$ only reaches 45% good detections of both moderate and strong belt looseness, while the raw indicator $\lvert \mathrm{IF}(f_r) \rvert$ barely detects 20% of belt looseness. This point shows the advantage of the proposed method and confirms that the transient state is better to monitor belt looseness.

It can be noticed in Fig. 9 that different indicators mainly react for sectors with higher load conditions (the right part of each zone) whatever the speed. The results of Tables IV and V reflect this fact, and it looks like nondetection are closely linked to low-load conditions. This is very coherent with Fig. 2 presented in Section III-A. The analysis of this figure showed that the relative belt slip increases with the load condition and that it remains almost the same for low-load conditions from I_0 to $I_n/2$. It can also be noticed from Tables IV and V that speed has only a little influence on results, except for low-torque conditions, where the detection is increased to 70% at speed Ω_5. So, it can be concluded that higher load conditions are better for diagnosis purposes. If it is not possible, high speed will be preferred for the diagnosis process.

The results obtained for a nonunitary transmission ratio (see Table VI) confirm the efficiency of the proposed indicator in terms of robustness and sensibility. The X_{CR} indicator reaches even a better detection rate with more than 98% strong belt looseness cases detected for only 1% false alarms. Contrariwise, the results obtained with the $\mathrm{IF}_{\mathrm{CR}}(f_r)$ indicator are rather disappointed. Even if its robustness is good (FA $= 0.4\%$), its detection rate is very low with only 6.6% belt looseness cases detected. This fact can be explained by the use of a bigger pulley on the driver side. It increases the adhesion surface on the pulley rotating at f_r. The signature obtained at this frequency are then less sensible to the belt slip.

VI. CONCLUSION

This paper presents an innovative method to monitor belt looseness through the analysis of phase currents. The analysis of belt slip under steady and transient states for different speed and load conditions helped to define relevant spectral signatures for the monitoring. The conclusion of this study is that the transient state is more appropriate for belt looseness detection because a sudden acceleration amplifies the relative belt slip. Accordingly, an original method is proposed based on the addition of a low square-wave component to a constant speed reference. This method allows us to periodically observe the impact of belt looseness on phase currents and then to process it as a Fourier series. The Fourier series coefficients are normalized and averaged in order to detect drifts that are statistically significant. This indicator is computed on the torque–speed plan according to an original technique in order to increase the robustness of the detection.

The proposed indicator is evaluated on an experimental test bench with an IM of 30 kW for moderate and strong belt looseness. Three different speeds and four different load conditions have been tested. The method reaches excellent results with almost 90% correct detections for 1% false alarms whatever the transmission ratio. As a comparison, indicators computed from the spectral analysis of phase currents under the steady state

reach barely 45% correct detections in the case of a 1:1 ratio. These results drop to 6.6% correct detections in the case of a nonunitary ratio. Moreover, the proposed method is robust to torque and speed changes even for low-load conditions, thanks to the torque–speed segmentation, and the threshold detection can be *a priori* chosen, thanks to the normalization process.

This method shows interesting results and confirms that the transient state is better for belt looseness monitoring. It has been demonstrated that high-load conditions must be privileged for diagnosis purposes. Future work will explore the use of other indicators, such as the phase, in addition of the signature amplitude in order to classify the fault severity and to propose a visual tool for the monitoring of belt looseness. Finally, this technique needs to be evaluated for other kind of faults or applications in order to evaluate if it enables fault discrimination.

Acknowledgment

The authors would like to thank H. Egreteau from Leroy Somer for his precious help and advices during the experimental tests carried out in this study as well as for the time he dedicated to perform them.

References

[1] M. Delgado, G. Cirrincione, A. G. Espinosa, J. A. Ortega, and H. Henao, "Dedicated hierarchy of neural networks applied to bearings degradation assessment," in *Proc. 2013 9th IEEE Int. Symp., Diagnostics Electr. Mach., Power Electron. Drives*, Aug. 2013, pp. 544–551.

[2] A. Picot, Z. Obeid, J. Régnier, S. Poignant, O. Darnis, and P. Maussion, "Statistic-based spectral indicator for bearing fault detection in permanent-magnet synchronous machines using the stator current," *Mech. Syst. Signal Process.*, vol. 46, no. 2, pp. 424–441, 2014.

[3] T. W. Rauber, F. de Assis Boldt, and F. M. Varejão, "Heterogeneous feature models and feature selection applied to bearing fault diagnosis," *IEEE Trans. Ind. Electron.*, vol. 62, no. 1, pp. 637–646, Jan. 2015.

[4] H. Razik, M. E. K. Oumaamar, and G. Clerc, "A hybrid kangaroo algorithm to assess the state of health of electric motors," in *Proc. 2013 9th IEEE Int. Symp., Diagnostics Electr. Mach., Power Electron. Drives*, Aug. 2013, pp. 43–48.

[5] A. Soualhi, G. Clerc, and H. Razik, "Detection and diagnosis of faults in induction motor using an improved artificial ant clustering technique," *IEEE Trans. Ind. Electron.*, vol. 60, no. 9, pp. 4053–4062, Sep. 2013.

[6] M. Y. Kaikaa, M. Hadjami, and A. Khezzar, "Effects of the simultaneous presence of static eccentricity and broken rotor bars on the stator current of induction machine," *IEEE Trans. Ind. Electron.*, vol. 61, no. 5, pp. 2452–2463, May 2014.

[7] K. H. Kim, "Simple online fault detecting scheme for short-circuited turn in a PMSM through current harmonic monitoring," *IEEE Trans. Ind. Electron.*, vol. 58, no. 6, pp. 2565–2568, Jun. 2011.

[8] F. R. Blánquez, C. A. Platero, E. Rebollo, and F. Blánquez, "Evaluation of the applicability of FRA for inter-turn fault detection in stator windings," in *Proc. 2013 9th IEEE Int. Symp., Diagnostics Electr. Mach., Power Electron. Drives*, Aug. 2013, pp. 177–182.

[9] B. Aubert, J. Régnier, S. Caux, and D. Alejo, "Kalman-filter-based indicator for online interturn short circuits detection in permanent-magnet synchronous generators," *IEEE Trans. Ind. Electron.*, vol. 62, no. 3, pp. 1921–1930, Mar. 2015.

[10] S. McInerny and Y. Dai, "Basic vibration signal processing for bearing fault detection," *IEEE Trans. Educ.*, vol. 46, no. 1, pp. 149–156, Feb. 2003.

[11] S. Djurović, D. Vilchis-Rodriguez, and A. C. Smith, "Vibration monitoring for wound rotor induction machine winding fault detection," in *Proc. XXth Int. Conf. Electr. Mach.*, Sep. 2012, pp. 1906–1912.

[12] J. Harmouche, C. Delpha, and D. Diallo, "A global approach for the classification of bearing faults conditions using spectral features," in *Proc. IECON 2013-39th Annu. Conf. IEEE, Ind. Electron. Soc.*, Nov. 2013, pp. 7352–7357.

[13] M. E. H. Benbouzid, "A review of induction motors signature analysis as a medium for faults detection," *IEEE Trans. Ind. Electron.*, vol. 47, no. 5, pp. 984–993, Oct. 2000.

[14] M. Riera-Guasp, J. A. Antonino-Daviu, and G. A. Capolino, "Advances in electrical machine, power electronic, and drive condition monitoring and fault detection: State of the art," *IEEE Trans. Ind. Electron.*, vol. 62, no. 3, pp. 1746–1759, Mar. 2015.

[15] A. Picot, D. Zurita, J. Cariño, E. Fournier, J. Régnier, and J. A. Ortega, "Industrial machinery diagnosis by means of normalized time-frequency maps," in *Proc. IEEE 10th Int. Symp., Diagnostics Electr. Mach., Power Electron. Drives*, Sep. 2015, pp. 158–164.

[16] H. Yamashina, S. Okumura, and I. Kawai, "Development of a diagnosis technique for failures of V-belts by a cross-spectrum method and a discriminant function approach," *J. Intell. Manuf.*, vol. 7, no. 1, pp. 85–93, 1996.

[17] G. Gerbert, "Belt slip—A unified approach," *J. Mech. Design*, vol. 118, no. 3, pp. 432–438, Sep. 1996.

[18] K. Seyfert, "Belt maintenance," *Motor*, p. 41, May 2004.

[19] H. P. Bloch and F. K. Geitner, "Installation and maintenance of v-belt drives," in *Major Process Equipment Maintenance and Repair* (ser. Practical Machinery Management for Process Plants), vol. 4, H. P. Bloch and F. K. Geitner, Eds. Houston, TX, USA: Gulf, 1997, pp. 310–328, ch. 7. [Online]. Available: http://www.sciencedirect.com/science/article/pii/S1874694297800090

[20] E. Fournier, A. Picot, J. Regnier, C. Andrieux, J. Saint-Michel, and P. Maussion, "Effects of transmission belt looseness on electrical and mechanical measurements of an induction motor," in *Proc. IEEE 10th Int. Symp., Diagnostics Electr. Mach., Power Electron. Drives*, Sep. 2015, pp. 259–265.

[21] A. Hazan, M. Verleysen, M. Cottrell, and J. Lacaille, "Probabilistic outlier detection in vibration spectra with small learning dataset," in *Proc. Int. Conf. Surveillance*, 2011.

[22] E. Fournier, A. Picot, J. Régnier, P. Maussion, M. TientcheuYamdeu, and J. M. Andréjak, "A generic diagnosis protocol for the monitoring of induction motors based on multiple statistical references in the torque-speed plane," in *Proc. 40th Annu. Conf. IEEE Ind. Electron. Soc.*, Oct. 2014, pp. 3348–3354.

[23] M. Blodt, M. Chabert, J. Regnier, and J. Faucher, "Mechanical load fault detection in induction motors by stator current time-frequency analysis," *IEEE Trans. Ind. Appl.*, vol. 42, no. 6, pp. 1454–1463, Nov./Dec. 2006.